Ecosystems
https://doi.org/10.1007/s10021-022-00769-2

Biophysical Heterogeneity, Hydrologic Connectivity, and Productivity of a Montane Floodplain Forest

Marc Peipoch,[1]* Pete B. Davis,[2] and H. Maurice Valett[2]

[1]*Stroud Water Research Center, Avondale, Pennsylvania, USA;* [2]*Division of Biological Sciences, University of Montana, Missoula, Montana, USA*

ABSTRACT

Floodplains display exceptional variation in habitat type, connectivity, and vegetation structure that make them ideal landscapes in which to address biophysical controls on primary production. However, our ability to do so requires fine-scale assessment of biophysical complexity over large spatial gradients in habitat heterogeneity, species composition, and productivity. We used LiDAR data and hydrologic modeling to quantify surface elevation, hydrologic connectivity, and a vegetation structural diversity index (VSDI) in 551 patches across a floodplain forest of a montane river corridor. We also estimated terrestrial primary production via the normalized difference vegetation index (NDVI) in each floodplain patch. Our main goal was to compare abiotic and biotic controls on terrestrial primary production using a path analysis model to estimate direct and indirect effects on NDVI values. Across the floodplain, patch inundation was predominantly low and negatively related to mean patch elevation ($r = -0.434$, $p < 0.001$) and distance to the river channel ($r = -0.397$, $p < 0.001$). Most patches exhibited high VSDI, corresponding to a total canopy cover of 25–65% and an average canopy height of 8.5 m. Path analysis revealed direct effects of inundation on canopy cover and NDVI, indicating abiotic control on both floodplain vegetation distribution and productivity. Canopy cover mediated indirect effects of inundation on vegetation structural diversity, which was in turn a strong mediator of the effects of canopy cover on forest productivity. Our results suggest that coexisting layers of vegetation in a floodplain patch provide complementary functional traits that interact with flooding regime to collectively increase aboveground productivity.

Key words: river-floodplain connectivity; habitat heterogeneity; diversity; NDVI; productivity.

HIGHLIGHTS

1. Aboveground productivity was robustly related to biophysical complexity across floodplain patches.
2. Floodplain inundation associated with river flood pulses exerts direct and indirect control on both structural diversity and productivity of floodplain vegetation.

Received 14 July 2021; accepted 5 May 2022

Supplementary Information: The online version contains supplementary material available at https://doi.org/10.1007/s10021-022-00769-2.

Author Contributions: All authors contributed significantly to conceive and design the study. PBD performed the research and analyzed data. MP contributed to data analysis and performed structural equation modeling. All authors contributed significantly to the redaction of the paper.

**Corresponding author; e-mail:* mpeipoch@stroudcenter.org

3. Coexisting layers of vegetation in floodplain habitats provide complementary strategies of resource use that interact with flooding regime to collectively increase aboveground productivity.

INTRODUCTION

Significant exchange of water, energy, and materials between rivers and floodplains has urged aquatic ecologists to think ‘outside the channel’ (Helton and others 2011) and forced forest managers to consider river flows (Rood and others 2005) when addressing forest ecosystems dynamics. Rivers are now increasingly recognized as corridors, combining channel and floodplain within the same ecosystem boundaries (Wohl and others 2017; Pettit and others 2017). Integration of the active channel and floodplain as a unique ecosystem through which energy and materials flow interchangeably is conceptually well developed (Records and others 2016; Wohl and others 2017), yet there remains a paucity of quantitative observations on aquatic-terrestrial linkages at the corridor scale (for example, Luck and others 2010) and their implications for river-floodplain systems. Better quantitative assessment of river-floodplain linkages should prove helpful in terms of theoretical considerations and because river corridors foster great biodiversity and support extensive ecosystem services (Tockner and Stanford 2002; Naiman and others 2005).

In their natural state, floodplains are a diversified mixture of aquatic and terrestrial habitats, constantly and rapidly changing over space and time with implications for habitat heterogeneity and connectivity. Habitat heterogeneity results from complex interactions among large wood (Latterell and others 2006), sediment load (Bechtold and Naiman 2009), flooding regime (Arscott and others 2000), and plant succession (Jansson and others 2000; Naiman and others 2010). Connectivity, *per contra*, is mostly related to the degree of flooding (Ward and others 2002). Seasonal inundation of floodplains, that is, the flood pulse (Junk and others 1989), delivers aquatic-derived subsidies of nutrients and water to floodplain forests, generally enhancing their productivity relative to upland forests (Megonigal and others 1997). However, flooding frequency and duration can vary significantly among patches of heterogeneous floodplains (Amoros and Bornette 2002). While periodic flooding can increase rates of primary production, long-term inundation may lead to anoxia and decrease productivity (Odum and others 1979). Changes in plant community structure and productivity occur mostly through the varying elevation of habitats on the floodplain and the river’s flooding regime (Johnson and others 2016).

Previous research has examined processes linking habitat heterogeneity and hydrologic connectivity to species composition of forested floodplains in temperate regions (Bornette and others 1998; Naiman and others 2010; Johnson and others 2016). Cottonwood (*Populus* spp.) recruitment to gravel bars is highly dependent on the timing and pace of flow recession in early summer (Mahoney and Rood 1998). In tropical floodplains, Wittmann and others (2006) explained tree species distribution only from changes in floodplain elevation and flooding frequency. Much less is known about how habitat heterogeneity and connectivity influence ecosystem functions such as primary production. Some have measured direct increases in productivity of entire floodplain forests as a result of periodic flooding, and attributed it to the increasing supply of water and nutrients from the river (Robertson and others 2001; Fonseca and others 2019). In addition to abiotic influences, changes in plant species composition may also affect variation in aboveground primary production. Species effects are known to interact with abiotic controls (resource supply, disturbance frequency, and so on) to determine ecosystem function (Hooper and others 2005). Whether abiotic and biotic effects on ecosystem properties are mutually exclusive, competing, or interactive has implications that go well beyond river corridors and extend to the overall effects of biodiversity on ecosystem function. Riverine floodplains are ideal landscapes in which to address these issues (Tockner and others 2010).

Diversity and Productivity in Floodplain Forests—Fine-scale Assessment of Broad Scale Patterns

Positive effects of species richness on primary production have been repeatedly reported over decades (Naeem and others 1994; Naeem and others 1996; Tilman and others 1996; Tilman and others 1997). Most studies suggest increases in functional diversity along with taxonomic richness as a mechanism for such ecosystem effects (Hooper and others 2005). For instance, floodplain patches developing woody vegetation may experience a shift in dominant functional traits such as average rooting depth or water demand that can likely influence local biodiversity and productivity. Biota within these habitats may even become less dependent on river-borne subsidies (that is, abiotic control) once woody vegetation is well established. River corridors display a remarkable gradient in both habitat composition (for example, sandbars, abandoned channels, filled-in oxbows, and so on) and vegetation structure (for example, grassland, regenerating stands, mature forest, and so on) that make them appropriate landscapes in which to compare abiotic and biotic controls on primary production. However, such comparisons have been limited in part by the scarcity of methods that allow accurate fine-scale determinations over larger spatial gradients in geomorphic heterogeneity, species composition, and productivity of riverine corridors.

Modern advancements in remote sensing methods such as light detection and ranging (LiDAR) and multispectral imaging are now providing accurate tools to quantify floodplain elevation, channel extension, and inundation probability at high resolution and over large spatial extents (Mertes 2002; Lorang and others 2005; Whited and others 2007). Some studies have proposed approaches to summarize floodplain heterogeneity and connectivity into tractable univariate metrics (Papadimitriou 2002; Scown and others 2016). Others have employed LiDAR data to address variability in the three-dimensional distribution of canopy elements (that is, canopy structural complexity, Fahey and others 2015) as a measure of functional diversity based on modified Shannon–Wiener indices (Listopad and others 2015). These contemporary techniques and metrics provide the opportunity to address influential interactions among habitat heterogeneity, hydrologic connectivity, vegetation diversity, and floodplain forest productivity.

In the glaciated Rocky Mountain regions of North America, annual spring snowmelt drives predictable flooding of floodplain soils, supporting a deciduous-conifer forest community, and promoting numerous processes above and below ground (Valett and others 2014; Hauer and others 2016). Deciduous trees (*Populus* spp. and *Salix* spp.) dominate early-successional patches that are replaced by conifer-dominated communities as annual flooding ceases due to surface aggradation, river channels migrate, and habitat turnover commences (Whited and others 2007). At any given time, a heterogeneous mosaic of early to late-successional stages is found across the floodplain (Stanford and others 2005), resulting in spatial variation of vegetation structure and productivity at the patch scale. Using LiDAR data and hydrologic modeling, we quantified surface heterogeneity, connectivity, and structural diversity of aboveground vegetation in a floodplain forest associated with a free-flowing, montane river of Western Montana, USA. We then evaluated abiotic and biotic controls on terrestrial primary production via the normalized difference vegetation index (NDVI) derived from multispectral aerial images. We employed path analysis as a hypothesis-testing method to evaluate how biotic and abiotic controls interact to control terrestrial productivity. An initial simple model, including only independent effects of abiotic and biotic factors on NDVI variation, was first tested with collected data. The model was then modified as needed, via parsimonious incorporation of interaction effects between abiotic and biotic variables, until the best-fitted path analysis model was determined. The model provides a conceptual causal map among representative variables of habitat heterogeneity, hydrologic connectivity, and vegetation structure, and their influence on floodplain forest productivity.

METHODS

Study Site and Spatial Resolution

The study was conducted in a section of the Bitterroot River floodplain, Montana (6.75 km long by 1.75 km wide), representative of unregulated, gravel-bed river floodplains across the northwestern USA (Figure 1). Throughout the study site, snowmelt-driven floods inundate the floodplain every spring with little anthropogenic resistance. At the study area, the river has a drainage area of over 7000 km^2 and an average annual flow of 50 m^3 s^{-1}, with peak flows greater than 350 m^3 s^{-1} during vernal flooding. Vegetation across the floodplain is dominated by black cottonwood (*Populus trichocarpa*), ponderosa pine (*Pinus ponderosa*), and quaking aspen (*Populus tremuloides*) forests, with a variety of small trees and shrubs including alder (*Alnus incana* and *Alnus sinuata*), juneberry (*Amelanchier* spp.), wood's rose (*Rosa woodsii*), and other native and non-native grasses.

To assess spatial relationships between abiotic and biotic variables across the floodplain landscape, we established experimental units at the patch scale. Floodplain patches were defined as geographic portions characterized by high internal spectral and spatial homogeneity, but with potentially differing areas. A segmentation approach was used to delineate patches; segmentation is a remote sensing method that creates homogeneous image objects through pattern recognition of spectral and spatial information (Jensen 2004). In our segmentation approach, we employed 4-band, 1-m reso-

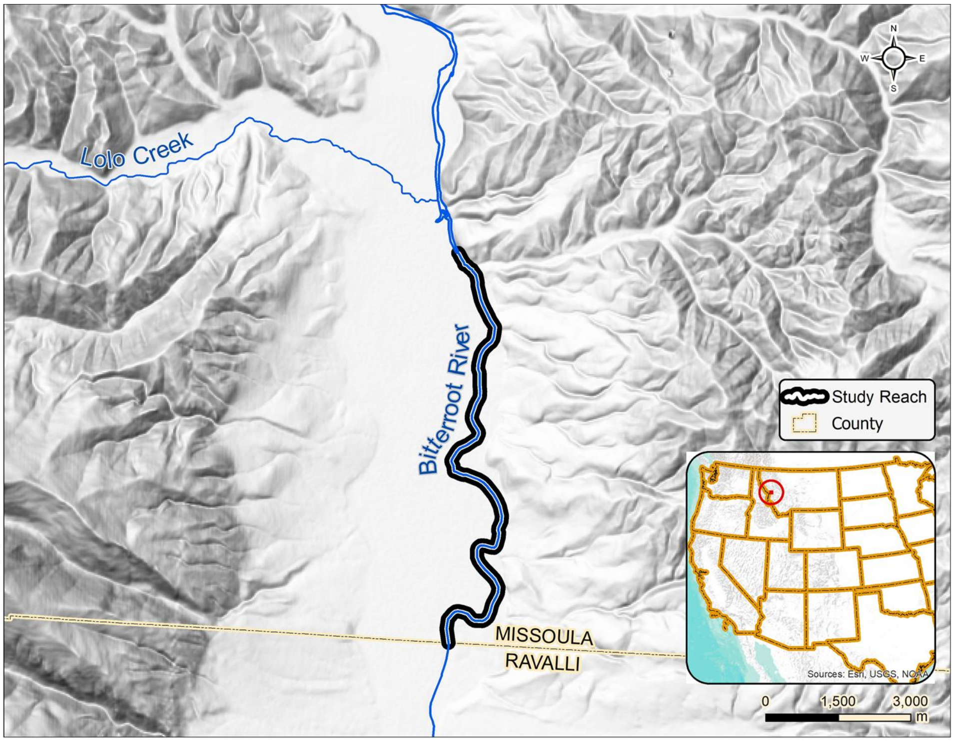

Figure 1. Elevation map showing the location of the study reach in the Bitterroot River valley. Inset shows the study site position in the northwest region of the USA. Dashed box illustrates spatial boundary of LiDAR data acquisition (see text for details).

lution imagery from the National Agriculture Imagery Program (NAIP) collected between June and September of 2013 to generate a single georeferenced layer composed of highly complex polygons (that is, patches). The layer included a total of 1311 patches. More than half were removed from further analysis for being outside the floodplain, intersecting water, or containing only riverside gravel beds devoid of vegetation. Ultimately, a total of 551 vegetated patches across the floodplain were retained for further quantitative analysis (Appendix 1A).

Surface Complexity, Vegetation Structural Diversity, and Primary Production

Measures of biophysical complexity, vegetation structure, and terrestrial productivity were derived from a variety of remotely sensed data. Physical complexity was characterized using a 0.4-m digital elevation model (DEM) generated from aerial LiDAR data acquired on September 9, 2016. Prior to computing any metrics, the DEM was detrended to remove the longitudinal gradient in elevation along the river corridor following methods described in Whited and others (2007). Surface heterogeneity among patches was characterized by comparing mean ground elevation of each patch. Surface heterogeneity within each patch was then estimated as the standard deviation of ground elevation (GESD).

Hydrologic connectivity of each patch was characterized by three metrics: mean flow length (FL), mean flow accumulation (FA), and percent inundation (PI). FL represents the length of a potential up-gradient flow path for each raster cell, and FA computes, for each cell within a patch, the cumulative number of cells (that is, total area) on a down gradient flow path that leads to it. Both FL and FA metrics were computed using a flow direction grid generated from the DEM according to the methods described in Jenson and Domingue (1988) and Tarboton and others (1991). Percent inundation (PI) was computed using an inundation raster generated from the DEM using the Hydrologic Engineering Center's River Analysis System (HEC-RAS), the HEC-GeoRAS ArcGIS extension, and the ArcGIS Arc Hydro package (HEC-GeoRAS 2012, HEC-RAS 2016, Arc Hydro 2015). A one-dimensional steady-flow model was used to simulate flooding effects at a river flow of 93.98 $m^3 s^{-1}$, which represents the daily average flow value between March-1 and August-1 over the 1990–2015 period using data from USGS gauging station 12352500 located downstream of our study site. This flow value does not represent the annual peak flow but the average river flow value throughout the annual growing season. Percent inundation (PI) was computed for each patch as the percent of the patch area covered by the inundation raster (Appendix 1B) and is interpreted as an indicator of the patch susceptibility to inundation during floodplain flooding.

Patterns of vegetation type and size across the floodplain were evaluated through the vegetative structural diversity index (VSDI) that uses the same approach as the Shannon–Wiener index for species diversity, but employs different data (Listopad and others 2015). Computation of VSDI values used point cloud elevation data derived from LiDAR non-ground points after normalizing by ground height. Four vertical height classes: 0 to 0.5 m, 0.5 to 2.5 m, 2.5 to 5 m, and $>$ 5 m were used in place of species richness (that is, $0 \leq S \leq 4$) representing the ground/herbaceous, shrub, young trees, and canopy trees layer, respectively. The proportion of total LiDAR point returns at each height class replaces the proportion of the patch occupied by each vegetation layer. With this approach, VSDI values equal or near zero reflect sparse vegetation cover and VSDI values increase as the distribution of LiDAR point density becomes more evenly distributed across the four height classes. We estimated patch canopy cover from LiDAR data using the standard formula of the ratio of the number of first returns above 2.5 m divided by the total number of first returns (McCallum and others 2014). We also used LiDAR point density to assess relatively mature vegetation and address successional progression of floodplain forest patches. Patches were categorized as belonging to early-, mid-, and late-successional stages based on canopy cover above 10 m height of $<$ 10%, 10–50%, and $>$ 50%, respectively. To relate structure-defined successional stages to differences in the dominant plant communities on the floodplain, we joined vegetation class attributes from the US Forest Service (USFS) Bitterroot National Forest mid-level (approximately 1:100,000) existing vegetation map (Ahl and Brown 2017) with the patches delimited in our study. The USFS vegetation map was developed using a similar segmentation approach to ours, and the segments were classified with dominant vegetation types. We maximized overlap between vegetation class and LiDAR data by using a spatial join in which the most overlap existed between segments.

The normalized difference vegetation index (NDVI) was used as a proxy for terrestrial productivity and was calculated from the same 2013 NAIP 4-band imagery used in the segmentation. NDVI is a widely used remotely sensed vegetation index that correlates well with biomass production (that is, net biomass increment), absorbed photosynthetically active radiation (APAR), leaf area index (LAI), percent canopy cover, and leaf chlorophyll levels (Tucker 1979; Lillesand and others 2015). Transformation of NDVI values to any specific measure of productivity was not possible due to the limited spatial scale of our study site that precludes the use of look-up tables that were developed at regional and global scales (Running and others 2004). NDVI values were calculated using reflectance values in the near-infrared and red bands via Eq. (1):

$$\mathrm{NDVI} = \frac{\rho\mathrm{NIR} - \rho\mathrm{RED}}{\rho\mathrm{NIR} + \rho\mathrm{RED}} \tag{1}$$

where ρNIR is the proportion of reflectance absorbed in the near-infrared (NIR) region of the electromagnetic spectrum, ρRED is the proportion of reflectance absorbed in the red region of the electromagnetic spectrum. NDVI output values range between -1 and 1, with greater values representing greater biomass production (Jensen 2004). Mean NDVI values derived from the pixels within each patch were used for further data analysis.

Data Analysis

Spatial variation of each metric across the floodplain was evaluated using kernel density plots that allow rapid assessment of distribution and central tendencies of observed values. Density probability distributions were generated using ‘geom_density’ function of the *ggplot2* package in the R environment (R Development Core Team 2008). Differences in vegetation structure and NDVI among successional stages were addressed using one-way ANOVA on ln-transformed data followed by Student–Newman–Keuls multiple comparison tests. Pairwise relationships between variables were assessed using Pearson product-moment correlations or regression models. Statistical difference were assessed with $\alpha = 0.05$.

To address how complex interactions among abiotic and biotic factors influence terrestrial productivity across floodplain patches, we employed structural equation modeling (Hershberger 2001). Specifically, we performed path analysis modeling, a form of structural equation modeling in which all variables are empirically represented (that is, models did not include latent variables). Path analysis is a useful technique for evaluating the fit of a proposed set of direct and indirect relationships to the observed data (Quinn and Keough 2002). We first used the 'lavaan' function of the *lavaan* package (Rosseel 2012) to fit an 'initial' direct model that included abiotic (PI) and biotic (canopy cover, VSDI) metrics via their individual (non-interactive) effects on terrestrial production (that is, NDVI). Then, we built six other models including different and distinct sets of individual and interactive effects among abiotic and biotic parameters including: only indirect abiotic effects on NDVI with mediation by both biotic variables (model 2), direct and indirect abiotic effects on NDVI with mediation by both biotic variables (model 3), only VSDI mediating abiotic effects on NDVI (model 4), only canopy cover mediating abiotic effects on NDVI (model 5), canopy cover mediating abiotic and VSDI effects on NDVI (model 6), VSDI mediating abiotic and canopy cover effects on NDVI (model 7). In all models, the effects of patch elevation, FL, and FA were only included as direct relationships to PI, but not as direct effects on biological parameters (canopy cover, VSDI, and NDVI) since we have no theoretical basis to support such linkage that is not explained by their influences on PI. All models included residual variance estimates for the dependent variables in the model, and models using canopy cover and VSDI variables without direct relationship between them also included a covariance term for their residuals to account for the strong correlation between them. Fit for each model was assessed using the standardized root mean square residual (SRMR) for which values < 0.05 are considered indicative of a good fit (Fan and others 2016). In some occasions, especially when sample size is limited ($N < 200$), SRMR can provide a biased assessment of model fit. Therefore, we employed two additional measures of model fit, the comparative-fit index (CFI) and the Tucker–Lewis index (TLI) indices. These metrics assess fit relative to a null model (that is, no relationships), are less affected by sample size, and provide more robust model assessment. Values greater than 0.95 of both CFI and TLI are considered indicative of good model fit. Our final path analysis model was selected by assessing Vuong test results (Vuong 1989) in the *nonnest2* package for all pairwise model comparisons including our initial direct-effects model and the six additional models with indirect effects. For the selected model, standard errors of unstandardized parameters were estimated by 1000 bootstrapped simulations to ease comparison among path coefficient in the model (standardized parameters vary only between –1 to 1). The roles of biotic variables as mediator variables (that is, existing measures that carry the influence of a given independent variable to a specified dependent variable) reflect indirect causality and were identified via the Sobel test (Sobel 1982).

RESULTS

Surface Heterogeneity and Hydrologic Connectivity

Patch size and shape varied across the floodplain with a predominance of smaller patches (Appendix 1A). Mean patch area was 1.34 ha, but patch size ranged more than an order of magnitude from as small as 0.11 to 8.35 ha. Mean patch perimeter to area ratio was 0.12 m^{-1} with values ranging an order of magnitude (0.04–0.46 m^{-1}). Mean patch elevation varied from 1.1 m below to 6.3 m above the floodplain average; high-elevation patches were exclusively located near the eastern hillslope. High-elevation patches, however, also encompassed substantial variation in surface elevation with GESD significantly correlated with patch elevation ($r = 0.605$, $p < 0.001$, Table 1). More than 95% of the patches exhibited low to moderate surface heterogeneity (GESD < 1.5 m), broadly distributed across both sides of the active channel (Figure 2A). The extent of variation in elevation within patches declined with distance from the active channel, but distance explained little of the variation in GESD ($r = -0.175$, $p < 0.001$, Table 1). Surface heterogeneity was also negatively but poorly related to patch area and perimeter to area ratio (Table 1).

Flood modeling showed that the flood pulse followed relict channels across the floodplain (Appendix 1B) and illustrated great variation in the proportional area per patch susceptible to inundation (Figure 2B). PI distribution revealed that few patches displayed extensive proportional inundation (4 patches with PI $> 80\%$), and most had much lower PI values. Average patch PI was 15%, and half of all patches were characterized by values equal to or lower than 20% (Figure 2B). Inundation extent was greater in low-elevation patches near the stream channel as indicated by negative correlations between PI and patch elevation ($r = -0.434$, $p < 0.001$, Table 1) and distance to the active channel ($r = -0.397$, $p < 0.001$). Most of the floodplain study area was poorly connected to the river during flooding (Figure 2B). Measures of floodplain linkages among patches (FL, FA) illustrated that most patches were poorly connected

Table 1. Correlation Coefficients for each Relationship Between Geographic, Topographic, and Connectivity Metrics

	Area	P/A	Distance	Elevation	GESD	PI	FL	FA
Area								
P/A								
Distance	-0.18^{***}	0.06						
Elevation	-0.03	0.06	0.10^{*}					
GESD	-0.05^{*}	0.02	-0.17^{***}	0.60^{***}				
PI	0.13^{***}	0.03	-0.40^{***}	-0.43^{***}	0.59^{***}			
FL	0.06	0.02	0.10^{**}	-0.05	-0.01	0.33^{***}		
FA	0.18^{***}	0.02	-0.01	-0.03	-0.09^{**}	0.40^{***}	0.85^{***}	

PI percent inundation; FL flow length; FA flow accumulation; P/A perimeter to area.
Statistical significance is indicated as p-value $< 0.05^{*}$, $< 0.01^{**}$, *and* $< 0.001^{***}$.

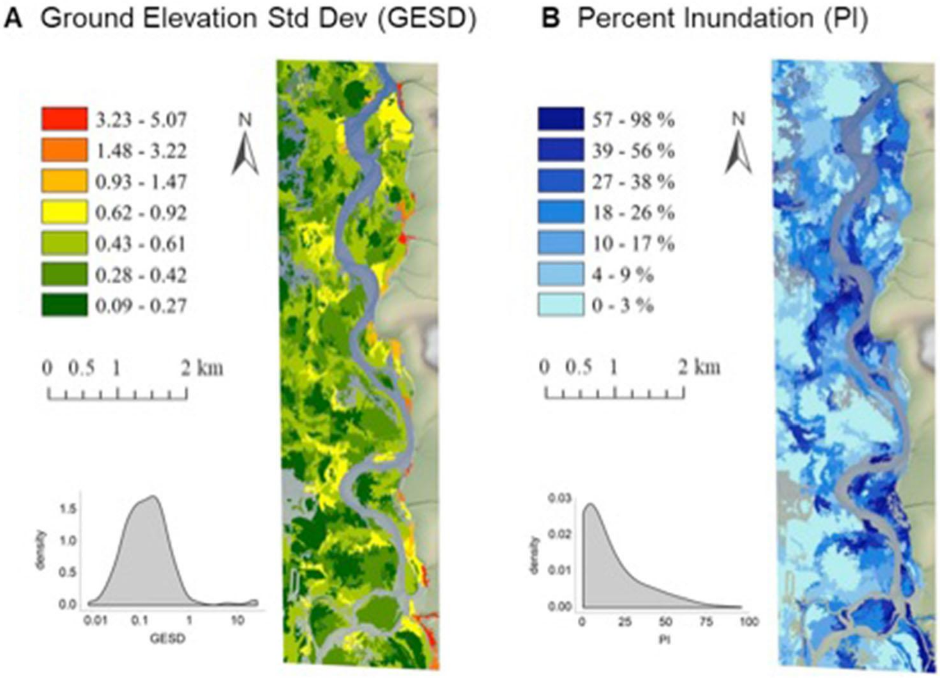

Figure 2. Map of ground elevation standard deviation (GESD) **A** and percent inundation (PI) **B** among floodplain patches. Individual patches were delineated by segmentation analysis. Values are color-coded in seven categories across the observed range. A kernel density plot showing the continuous distribution of each variable across the floodplain is shown at the bottom left part of each panel.

compared to a subset of patches with much higher FL and FA values (Appendix 2). Specifically, less than 5% of the patches showed potentially high hydrologic connectivity, with flowpaths (that is, FL values) of 25 m or more and contributing areas (that is, FA values) greater than 1.15 hectares.

Vegetation Structural Diversity in the Floodplain Landscape

Variation in canopy structural complexity (that is, VSDI) exhibited a moderately left-skewed distribution throughout the floodplain with range from 0 to 1.35 and a median value of 0.78 (Figure 3), congruent with a predominantly forested landscape. More than half of the patches exhibited VSDI values between 0.7 and 1, corresponding to canopy cover of 25–65% and an average canopy height of 8.5 m. Patches with low VSDI values (0–0.21; Figure 3), characteristic of grassland-dominated environments, represented approximately 10% of all patches.

As intended, the extent of mature canopy (that is, above 10 m height) increased significantly

(ANOVA, $p < 0.0001$) across successional stages (Table 2). Similarly, percent total cover increased significantly from 5.6 to 40 and 66.3% across early-, mid-, and late-successional stages (Table 2). Grass and shrub were 2 to 10 times more abundant in early succession patches than in mid- and late-successional stages, while ponderosa pine were similar in early and mid-stages but very scarce in late-successional patches (Appendix 3). Cottonwoods (Populus spp.) dominated plant communities in both mid- and late-successional stages across the floodplain (Appendix 3). Herbaceous communities were only dominant in patches characterized as early-successional stages (low VSDI), in contrast to tree communities being the dominant vegetation growth forms in mid- to late-successional stages (Appendix 4). VSDI was related to cover above 10 m height (Figure 4A) following an exponential rise to a maximum ($r2 = 0.64$, $p < 0.0001$), and increased with total canopy cover (Figure 4B) as a power law (log-VSDI vs. log-CC; $r2 = 0.94$, $p < 0.001$) with VSDI increasing more rapidly from early- to mid- than from mid- to late- successional stages (Figure 4). Accordingly, mean VSDI was significantly lower (ANOVA, $p < 0.0001$) in early-successional patches (0.27) than in later stages, but average values did not differ between mid (0.80) and late (0.82) stages (Table 2).

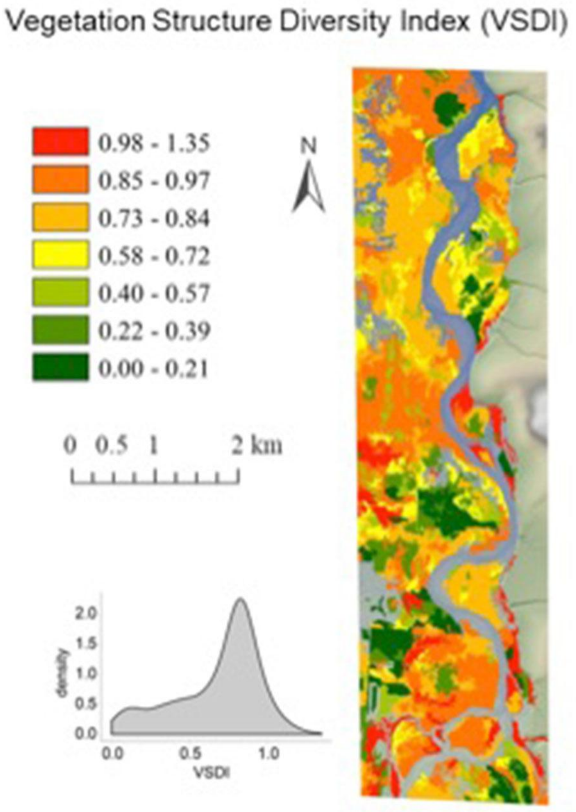

Figure 3. Map of vegetation structural diversity index (VSDI) across floodplain patches. Values are color-coded in seven categories across the observed range. A kernel density plot showing the continuous distribution of each variable across the floodplain is shown at the bottom left of the figure.

At the same time, variation in all structural metrics was an order of magnitude greater among early-successional patches than for later stages of succession (Table 2). Variation in mature (that is, > 10 m) and total canopy coverage was similarly high during early succession (CV = 76.8 and 86.3%, respectively) and then fell to less than 6% for both metrics during mid and late succession (Table 2). For VSDI, CV declined from 1156.6 to 148.4 and 127.9% across successional stages (Table 2, Figure 4). Thus, although greatest mean values for VSDI occurred during mid- and late-successional stages (Table 2), 7 of 35 VSDI values (20%) in excess of 1.0, were observed in early-successional patches, contributing to the observed degree of variation. In addition, the remaining 80% of VSDI values greater than one occurred among mid-successional patches (Figure 4). Thus, greater VSDI values did not necessarily entail more densely developed high profile mature canopies (that is, those with maximal late-successional character),

Table 2. Vegetation Canopy Characteristics Among Successional Stages

Successional stage	% Cover above 10 m		Total cover (%)		VSDI		NDVI	
	Mean	CV (%)	Mean	CV (%)	Mean	CV (%)	Mean	CV (%)
Early	2.7^{A}	76.8^{A}	5.6^{A}	86.29^{A}	0.27^{A}	1156.6^{A}	-0.06^{A}	1926.3^{A}
Mid	28.2^{B}	5.3^{B}	40.0^{B}	3.6^{B}	0.80^{B}	148.4^{B}	0.11^{B}	950.6^{B}
Late	56.8^{C}	1.9^{C}	66.3^{C}	1.6^{C}	0.83^{B}	127.9^{C}	0.26^{C}	416.6^{C}

*Within a column, metrics with different superscripts are statistically different across successional stages. Differences among mean values reflect significant ANOVA ($p < 0.0001$) followed by Student–Newman–Keuls multiple comparison tests. Variance within groups is represented by the coefficient of variation (CV; mean/standard deviation*100%), and significant differences in variances were determined by Levene's test ($p < 0.001$) for all comparisons. Analyses were run on ln-transformed data. Results shown here are back-transformed.*

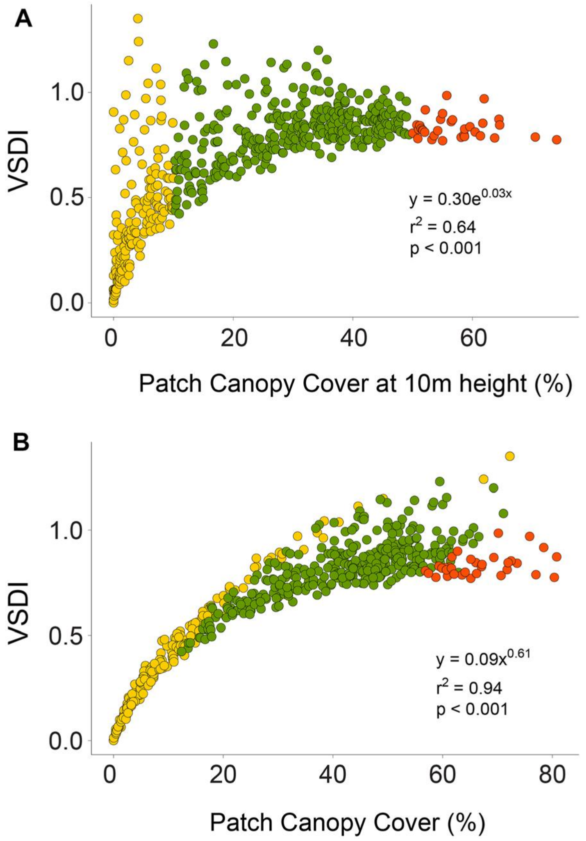

Figure 4. Relationship between mean vegetation structural diversity index (VSDI) and successional stage (that is, canopy cover above 10 m height) for individual plots **A** and total canopy coverage across all heights **B**. Colors are early- (yellow), mid- (green) and late- (red) successional designations.

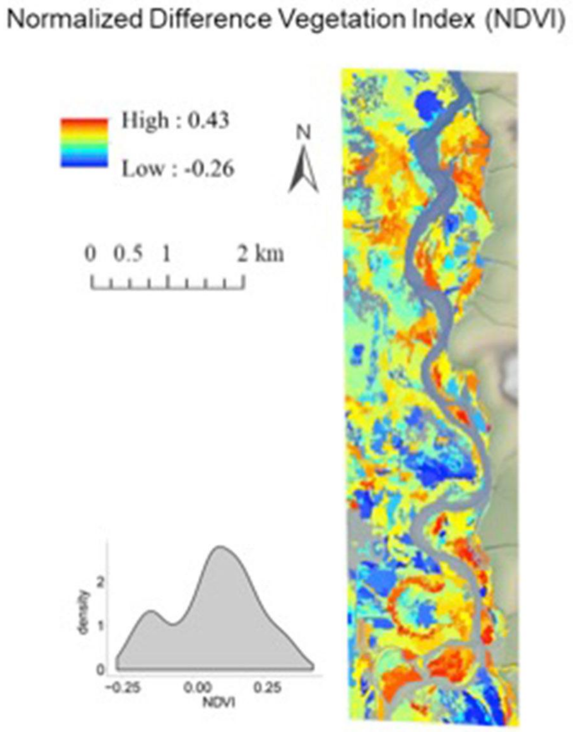

Figure 5. Map and kernel density plots for the normalized difference vegetation index (NDVI). Colors correspond to the provided gradient in NDVI intensity based on mean values for individual patches.

but instead were associated with substantial canopy development that included well-established understories, typically located among mid- and late-successional patches.

Abiotic and Biotic Effects on Floodplain Production

Across the floodplain, mean NDVI per patch varied from those indicative of bare earth (≤ 0), to a dominance of grass and sparse vegetation (0.0–0.25), or more densely forested patches (0.25–0.43; Figure 5). Negative NDVI values were observed for 155 patches (28% of total), indicative of recently disturbed patches. Across all patches, the grand mean for NDVI was 0.09 ± 0.15 ($\bar{x}$ ± standard deviation), generally reflecting a vegetated landscape. Average NDVI among vegetated patches (that is, those with positive NDVI values) was 0.15 ± 0.09 (Figure 5). Within successional stages, variation in NDVI was large with CVs ranging from 416.6 to 1926.3% (Table 2). Even with this broad variation, mean NDVI increased significantly (ANOVA, $p < 0.0001$) with succession from a negative average within early stages (−0.06) to progressively more positive values during mid (0.11) and late (0.26) succession (Table 2). Despite the extensive variation in both NDVI and VSDI among patches and successional stages, the two variables exhibited a strong positive relationship ($r = 0.69$, $p < 0.0001$, $n = 551$) across the floodplain (Figure 6), similar to the observed relationship between NDVI and canopy cover across the floodplain ($r = 0.71$, $p < 0.0001$, $n = 551$). Across successional development, however, the relationship between productivity and canopy structural diversity differed among stages (Table 2). Although variation in both NDVI and VSDI was extensive during early succession (that is, CV > 1000–2000%), the relationship remained significant ($r = 0.52$, $p < 0.0001$, $n = 175$) as it did among mid-successional patches ($r = 0.56$, $p < 0.0001$, $n = 343$). During late succession, however, patch NDVI was not related to structural diversity ($r = 0.11$, $p = 0.525$, $n = 33$) or total canopy cover ($r = 0.29$, $p = 0.094$, $n = 33$) suggesting

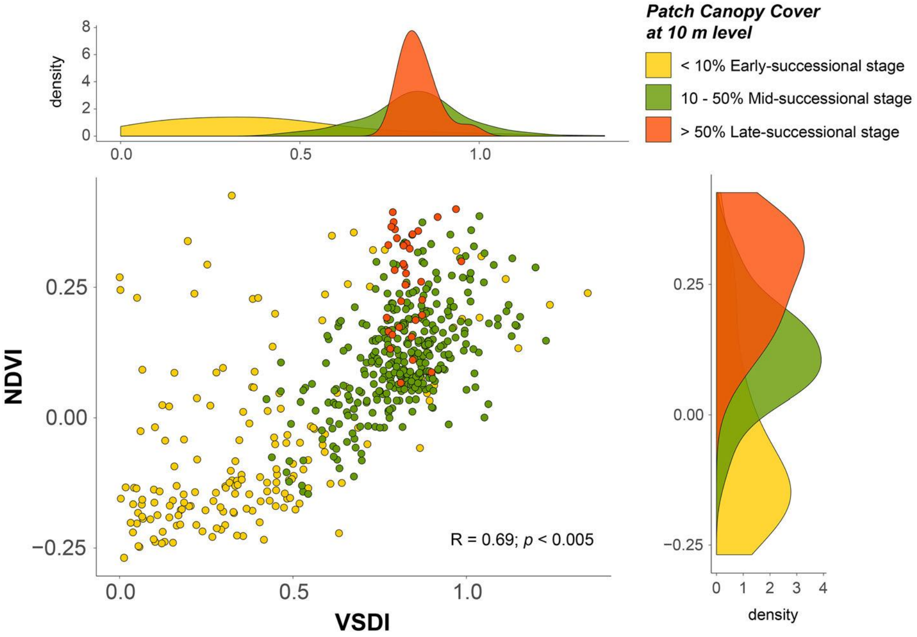

Figure 6. Normalized difference vegetation index (NDVI) versus vegetation structural diversity index (VSDI) across 551 floodplain forest patches. Panels on top and side of figure are kernel density plots relating to VSDI and NDVI, respectively. Symbol colors correspond to putative successional stages as designated by percent canopy cover above 10 m height.

a stronger interaction between vegetation structure and forest function during more actively growing conditions than at maturity.

Our initial path analysis model (Figure 7A), addressing only the direct and non-interactive effects of abiotic and biotic metrics on productivity, suggested that percent inundation, canopy cover, and structural diversity had direct effects on productivity. The model, however, was not well fitted to the observed data. All three indices employed to assess model fit indicated a large discrepancy between this initial model and the covariance matrix derived from our data (Figure 7B; SRMR = 0.278, CFI = 0.476, and TLI = 0.214). Our best-fit refined model (model 7; Figure 7C), as indicated by greatly improved indices (Figure 7D; SRMR = 0.048, CFI = 0.979, TLI = 0.955, and total model $R^2 = 0.538$), was obtained after removing flow path length due to poor contribution to explained PI variance, maintaining direct abiotic effects of PI on NDVI, and allowing VSDI to mediate the indirect effects of percent inundation and canopy cover on NDVI values (Figure 7C). The fit of model 7 was identical to model 6 and slightly better than models 4 and 5 (Appendix 5). We selected model 7 based on the stronger mediation of abiotic effects on vegetation structure and productivity by canopy cover than by VSDI. Results of Sobel tests confirmed the mediator role of canopy cover on the relationship between PI and VSDI (p-value < 0.001) and between PI and NDVI (p-value = 0.005), as well as the mediation of VSDI on the relationships between PI and NDVI (p-value = 0.028) and between canopy cover and productivity (p-value = 0.016; Figure 7C). Total indirect (mediated) effects on productivity correspond to the sum of all specific mediation paths from PI to NDVI, each one calculated as the product of its two standardized path coefficients. Summation of this type showed that indirect effects on productivity (0.259) were similar in magnitude to direct abiotic effects (0.257; Figure 7C), with canopy cover accounting for 77% (0.199) and VSDI representing 23% (0.060) of total indirect effects on NDVI. Indirect effects of PI on NDVI values were marginally mediated by VSDI (direct effects = 0.257; indirect effects = 0.020; Figure 7C), while this same abiotic effect was far more influentially routed through canopy cover as a much stronger mediator of productivity (direct effects = 0.257; indirect effects = 0.144; Figure 7C). In addition, patch canopy cover largely mediated the PI effects on VSDI values (direct effects = 0.080; indirect effects = 0.385; Figure 7C), indicating that canopy cover mediates inundation effects on both vegetation structure (VSDI) and productivity (NDVI). Mediation by VSDI was instead focused on how canopy cover drives productivity (direct effects = 0.343; indirect effects = 0.224; Figure 7C). Because direct effects of PI on VSDI are comparatively

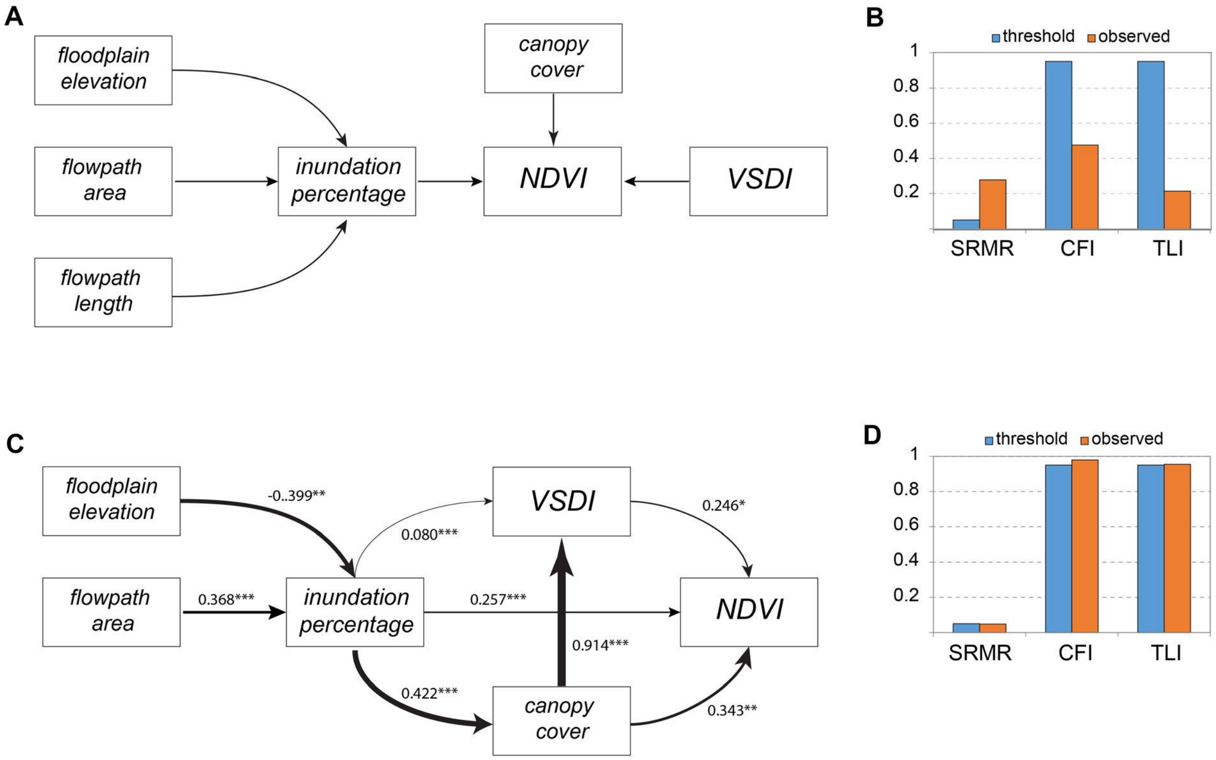

Figure 7. Initial path analysis model constrained to include all possible predictors and non-interactive effects of abiotic (ground elevation, flowpaths features, and inundation) and biotic (canopy cover, VSDI) factors on NDVI values **A** Criterion and observed values for fit indices associated with the initial model indicating poor model fit **B**. Strong fits are indicated by SRMR less than 0.05 and values for CFI and TLI greater than 0.95. Optimal parsimonious path analysis model including interactive effects **C** as assessed by SRMR, CFI, and TLI indices **D**. Standardized path coefficients provided in C indicate effect sizes used to compare relative magnitude of biotic and abiotic influences on NDVI values. Coefficients for residual covariance parameters are not shown for the sake of simplicity. Statistical significance of each unstandardized patch coefficient is indicated as p-value $< 0.05^{*}$, $< 0.01^{**}$, and $< 0.01^{***}$.

low, VSDI values do not appear constrained by inundation susceptibility, but instead, in combination with results from assessment of VSDI and NDVI among successional stages, vegetation structure appears to mediate the strength and slope of the relationship between canopy cover and productivity among successional stages (Table 2; Figures 6 and 7C).

Discussion

Structural diversity of vegetation varied across the floodplain, reflected large-scale patterns of flooding disturbance, and mediated abiotic influences on ecosystem function. Floodplain habitats near the channel or in other positions of low topographic elevation were more prone to extensive inundation by flooding of average magnitude. In turn, the inundated area within a patch was positively related to the presence of multiple levels of vegetation height and density of canopy cover. Flooding exposure was clearly linked to terrestrial productivity as seen in other floodplain forests (Clawson and others 2001; Naiman and others 2010; De Jager and others 2019; Fonseca and others 2019), but here its effects appear tightly mediated by the extent and structural diversity of vegetation development within patches. Asner and others (2014) characterized forest functional diversity as the interplay between phylogenetic traits of canopy trees along gradients of elevation and soil fertility that can ultimately influence ecosystem functioning. In our study, the use of a diversity metric quantifying vegetation layers rather than species richness illustrated a close association between structural diversity of vegetation and aboveground productivity. Together, the results suggest that functional characteristics of coexisting layers of vegetation in a floodplain patch provide complementary strategies of resource use that interact with flooding regime to collectively increase aboveground productivity.

Physical Heterogeneity Organizes Connectivity in Montane Floodplains

All floodplain patches will ultimately experience physical change, but many remain unaltered long enough for communities to be influenced by succession (Whited and others 2007; Driscoll and Hauer 2019). Our study focuses on the more acute roles of river flow and surface heterogeneity embedded within long-term floodplain evolution (for example, > 100 years, see Naiman and others 2010). The data presented here suggest that connectivity between the floodplain and its river depends largely on the location and topography of floodplain habitats, with implications for forest structure and productivity.

The Bitterroot River floodplain is a prime example of riverine landscapes in the Rocky Mountains (compare Stanford and others 2005; Hauer and others 2016) where an anastomosed river flows through gravel beds and fine sediment deposits in a floodplain of 1–2 km width. Average patch elevation across the floodplain varied in a similar range to that observed across the nearby Nyack floodplain of the Flathead River, MT (Whited and others 2007), was substantially greater than the 20–80 cm gradient organizing inundation in the Mississippi River floodplain (Swanson and others 2017), and less than the minimum 5-m range distinguish critical floodplain landforms in the Amazon lowlands (Asner and others 2014). Average and standard deviation of patch elevation were strongly and positively correlated, with greater surface heterogeneity (that is, GESD) in smaller patches near the river channel which may reflect the irregular topography of alluvial deposits of former channel migrations (Brunke and Gonser 1997; Lorang and others 2005). In their study of topographic complexity, Scown and others (2016) found that surface heterogeneity increases if measured at smaller sampling scales, and pointed out that floodplains with less than 2 km between valley slopes—as in our study site—present a more heterogeneous terrain compared to wider floodplains due to increased localized stream power. These perspectives seem generally applicable to the Bitterroot floodplain complexity.

Surface heterogeneity and hydrologic connectivity are mutually dependent, and thus, significant relationships between topographic metrics and connectivity indicators were expected a priori. However, only percent inundation (PI) was strongly related to patch elevation, GESD, and proximity to the river channel. Observed relationships between patch elevation and inundation in our study reflect connection to the main channel since PI was computed using a model relating river stage to surface elevation. Hence, inundation was more extreme in highly heterogeneous, low-elevation patches near the channel, reflecting overland flow to the floodplain during flood events. Braided and anastomosed channels can serve as conduits through which water and resources are distributed across floodplains (Malard and others 1999; Ward and others 1999), and changes in floodplain elevation naturally result in the modification of water surface elevation for a given river flow (Lane and others 2007; Lane and Thorne 2007). A measure of potential distance traveled by overland flow (FA) was positively related to PI, and it is reasonable to postulate that abandoned channels are contributing to flowpath area, connecting flooding waters from the channel to one or more floodplain patches.

Hydrologic Connectivity Drives Vegetation Productivity and Complexity

In the Bitterroot floodplain, the dependency of vegetative structural diversity on river-derived resources is focused on the effects of vernal flooding. Path analysis indicated that the susceptibility of patch area to inundation was directly related to canopy cover and most strongly indirectly related to structural diversity of terrestrial vegetation. These results suggest that the degree of connectivity between forest patches and the river channel during flooding is an important organizing factor determining vegetation structural diversity across the floodplain. To our knowledge, ours is the first study to relate habitat location and inundation to structural diversity of floodplain vegetation.

Previous research has described the implications of flood pulses for connecting aquatic resources to riparian plant diversity (Bornette and others 1998; Pollock and others 1998; Johnson and others 2016) and vegetation community development (Salo and others 1986; Whited and others 2007). However, flooding may also affect forest succession and structural diversity through legacy effects of channel migration. Asner and others (2014) showed that topographic filtering, resulting from the influences of distinct fluvial landforms on the Amazon floodplain, organized forest composition and conditions. Similarly, Naiman and others (2010) argued that the geomorphic legacy of flooding in coastal riparian forests of the Pacific Northwest sorted forest biomass and composition. Stella and others (2011) found that abandoned channels supported more than 50% of the extant cottonwood forest over a 160-km reach of the Sacramento River. In our study, many patches far from the river with high VSDI and NDVI values are shaped as forest polygons that resemble fluvial geomorphic features (for example, the oxbow in the southwest portion of the floodplain, Figs. 3 and 5). Thus, contemporary distribution of functional diversity reflects both acute influence of the current hydrograph and historical fluvial development of the floodplain surface.

The benefits of seasonal inundation for floodplain plant productivity have been extensively documented since Junk and others (1989) presented the flood pulse concept more than 30 years ago. However, prolonged flooding of floodplain soils can drastically change physical and chemical conditions (Clawson and others 2001) and influence plant species that may, or may not, be adapted to lengthy periods of saturation (Streng and others 1989; Battaglia and others 2000). Specifically, recurrent and extensive inundation may impede establishment of some woody plants, preventing forest succession while favoring sedges and wetland-like grasses (Bejarano and others 2020). In our study, PI was linearly and positively related to both canopy cover and VSDI of floodplain patches, suggesting that inundation associated with the flooding regime of the Bitterroot River does not correspond to a degree that prevents or retards forest development as frequently seen for bottomland forests (Megonigal and others 1997).

Inundation, Functional Diversity and Floodplain Productivity

One of the main goals in this study was the comparative assessment of abiotic and biotic controls on aboveground productivity and exploration of the role that vegetation structural diversity may play as a mediator of abiotic control of riparian forest productivity. The direct effects that patch inundation has on canopy cover and, to a lesser extent, on vegetative structural diversity represent abiotic control on floodplain vegetation distribution and abundance. However, path analysis also revealed additional effects of this abiotic driver to rates of terrestrial productivity (that is, NDVI), suggesting that inundation exerts direct control on both diversity and function of floodplain vegetation.

In this way, both canopy cover and vegetative structural diversity served as mediators linking abiotic hydrologic drivers to riparian plant productivity. Causal pathways linking water supply to enhanced abundance and biomass of vegetation have been reported for riparian forests of a diverse array of floodplains, including interior Alaska (Yarie 2008), Amazonia (Saatchi and others 2007), and the coastal plain of southeastern USA (Battaglia and Collins 2006), and in particular for water-limited systems characteristic of semi-arid landscapes (Lite and others 2005; Mac Nally and others 2011; Thevs and others 2012). Our study contrasts the direct influence of flooding on patch canopy cover with strong indirect effect on vegetation structural diversity; while laying out the importance of flooding for floodplain forest productivity via indirect pathways mediated by canopy cover and structural diversity. Others working mainly in upland forests have shown that canopy complexity increases above ground net primary productivity (Hardiman and others 2013; von Gadow and others 2016; Glatthorn and others 2018). Using a multiple linear regression model, Glatthorn and others (2018) estimated that structural complexity accounted for a 10% increase in net primary production in native beech forests. Similarly, the optimal path analysis model derived from our study assigned an increase in NDVI of approximately 0.07 units to the direct and indirect effects of canopy complexity, which in relation to the NDVI values observed, represents a 10.1% increase as well.

Although less work has addressed the structural complexity of floodplain forests, Acker and others (2003) reported that most measures of stand complexity were greater for upland forests than for those found along low- to mid-order streams. Most work on riparian forest complexity addresses its implications for adjacent streams. Keeton and others (2007) calculated a forest height diversity index similar to ours for riparian forests of the Adirondack Mountains, New York (USA), and linked it to the in-stream standing stocks of large woody debris and stream geomorphic structure. Warren and others (2016) argued that riparian canopy complexity influenced light regimes reaching streams, a proposal supported by work showing that horizontal forest structure was tied to below-canopy light availability along forested headwater streams (Siegloch and others 2017). In turn, Bechtold and others (2017) indicated that stream gross primary production increased with a proxy for riparian canopy complexity.

Functional Traits, Succession and Canopy Complexity

An understanding of how changes in community composition and vegetation structure can influence ecosystem properties requires an understanding of the functional traits of the species (Hooper and others 2002). The differing importance of the four layers of vegetation considered in our study represents evident change in canopy characteristics that reflects dominant functional traits and/or age of the species involved (Tilman and others 1997; Asner and others 2014). Moreover, the collective functional traits at the patch level impart a canopy complexity emerging from the different vegetation layers that is measured as foliage height diversity (aka VSDI). Others have emphasized the congruence between species composition and functional traits in forest ecosystems (Fahey and others 2015; Fotis and others 2018). In the Bitterroot's floodplain forest, the plant community ranges from bare ground/seedlings and tall grasses to shrub/willow and large trees (for example, cottonwoods, ponderosa pine). While mechanisms exist for individual plants to adjust vertical distribution of leaf mass and resources that can contribute to canopy complexity (Glatthorn and others 2018), differential recruitment success and growth rates within and among species likely plays a critical role in development of variation among height layers (Fotis and others 2018). Thus, high VSDI values do not necessarily reflect correspondingly large species diversity, but most likely indicate the presence of multiple, complementary life forms responding to resource availability and disturbance history. Our results support the role of increased functional diversity translating into greater productivity, suggesting that greater foliage height diversity emerges from niche differentiation within patch boundaries generated by spatial heterogeneity in surface elevation and flooding frequency.

For riparian forests, many have shown how succession can be strongly dependent on patterns of river flooding via surface connectivity (Keeton and others 2007; Driscoll and Hauer 2019). At the floodplain level, the relatively natural disturbance regime associated with cut-and-fill alluviation (Stanford and others 2005; Whited and others 2007) along the Bitterroot River continually creates new patches with unoccupied niches that allow establishment of grasses and seedlings leading to succession and the development of a full canopy. Many studies addressing the role of canopy complexity are framed in the context of succession. Most of these studies, however, have addressed more upland forests and emphasized the importance of enhanced structural diversity within and among old growth forests. Work by Hardiman and others (2011) showed that canopy complexity increased with successional stage, was linked to net primary production, and proposed its proliferation as a mechanism for the potential maintenance of productivity in aging forests. Similarly, Fahey and others (2015) found that canopy complexity was greater in older forests, but only when addressed at scales that incorporated disturbances, a condition representative of the shifting habitat mosaic characteristic of floodplains (Stanford and others 2005). On the other hand, Fotis and others (2018) showed that complexity was greatest in high-elevation early-successional plots and lowest for lower elevation plots with mid-successional species.

CONCLUSIONS

Results from our study lend to resolving competing models governing abiotic and biotic components of the flood pulse and its influences. One model addressing linkage among flooding, canopy complexity, and riparian forest productivity suggests that as succession proceeds, structural diversity increases rapidly associated with the extent and maturity of canopy formation. Once established, a full suite of vegetation layers with complementary patterns of resource use, coexist in a given patch increasing local rates of productivity. In this way, the abiotic forcing functions provided by the flood pulses are mediated by the extent of vegetative development. Alternatively, strong environmental filtering may limit species richness, restrict the range of adaptive traits, and constrain functional diversity and its biological effects on ecosystem properties. In this scenario, because environmental control overrides species effects on ecosystem properties, biotic mediation of abiotic effects is unlikely. This phenomenon has been observed in semi-arid floodplains where flooding alone emerges as the primary driver of floodplain vegetation productivity by stimulating production under wet conditions (Bunn and others 2006) and reducing it during dry periods (Parsons and Thoms 2013). Thapa and others (2016) proposed that semi-arid floodplains follow an adaptive cycle driven by flooding disturbance and relatively unaffected by community assembly. In high-latitude regions where water is not the limiting resource but nutrients are, the pulsatile input of aquatic-derived resources is known to alleviate nutrient limitation of riparian production regardless of forest composition (Naiman and others 2002; Schindler and

Smits 2017). For montane floodplains of the northwest USA, our results suggest that riparian productivity responds to flooding pulses as previously recognized, but this interaction is mediated among patches by the successional vegetation abundance and complexity rather than by solely abiotic linkage. Differences in the extent to which biotic mediation is central to floodplain vegetation dynamics may exist among bioclimatic regions reflecting more extreme fluctuation of wet-dry periods and more extensive nutrient limitation in arid or high-latitude regions, respectively.

ACKNOWLEDGEMENTS

The authors are grateful for the contributions of Lloyd Queen and Anne Klene to this research. Financial support was provided by the MPG Ranch, by NSF LTREB award (DEB 1655197) to HM Valett and M Peipoch and in part by the National Science Foundation EPSCoR Cooperative Agreement OIA-1757351. Insightful comments from two anonymous reviewers greatly improved the content and presentation of this manuscript.

DATA AVAILABILITY

Data can be found at https://github.com/mpstroud/BitterrootFloodplainRawData/blob/main/thesis_all data.csv.

Declarations

Conflict of interest The authors declare that they have no conflict of interest.

REFERENCES

Acker SA, Gregory S, Lienkaemper G, McKee WA, Swanson FJ, Miller SD. 2003. Composition, complexity, and tree mortality in riparian forests in the central Western Cascades of Oregon. Forest Ecology and Management 173:293–308.

Amoros C, Bornette G. 2002. Connectivity and biocomplexity in waterbodies of riverine floodplains. Freshwater Biology 47:761–776.

Arc Hydro (version 10.2). 2015. ESRI. http://resources.arcgis.com/en/communities/hydro/01vn0000000s000000.htm.

Arscott DB, Tockner K, Ward JV. 2000. Aquatic habitat diversity along the corridor of an Alpine floodplain river (Fiume Tagliamento, Italy). Archiv Fur Hydrobiologie 149:679–704.

Asner GP, Martin RE, Tupayachi R, Anderson CB, Sinca F, Carranza-Jimenez L, Martinez P. 2014. Amazonian functional diversity from forest canopy chemical assembly. Proceedings of the National Academy of Sciences of the United States of America 111:5604–5609.

Battaglia LL, Collins BS. 2006. Linking hydroperiod and vegetation response in Carolina bay wetlands. Plant Ecology 184:173–185.

Battaglia LL, Fore SA, Sharitz RR. 2000. Seedling emergence, survival and size in relation to light and water availability in two bottomland hardwood species. Journal of Ecology 88:1041–1050.

Bechtold HA, Rosi EJ, Warren DR, Keeton WS. 2017. Forest Age Influences In-stream Ecosystem Processes in Northeastern US. Ecosystems 20:1058–1071.

Bechtold JS, Naiman RJ. 2009. A Quantitative Model of Soil Organic Matter Accumulation During Floodplain Primary Succession. Ecosystems 12:1352–1368.

Bejarano MD, Sordo-Ward A, Alonso C, Jansson R, Nilsson C. 2020. Hydropeaking affects germination and establishment of riverbank vegetation. Ecological Applications 30.

Bornette G, Amoros C, Lamouroux NL. 1998. Aquatic plant diversity in riverine wetlands: The role of connectivity. Freshwater Biology 39:267–283.

Brunke M, Gonser T. 1997. The ecological significance of exchange processes between rivers and groundwater. Freshwater Biology 37:1–33.

Bunn SE, Thoms MC, Hamilton SK, Capon SJ. 2006. Flow variability in dryland rivers: Boom, bust and the bits in between. River Research and Applications 22:179–186.

Clawson RG, Lockaby BG, Rummer B. 2001. Changes in production and nutrient cycling across a wetness gradient within a floodplain forest. Ecosystems 4:126–138.

De Jager NR, Van Appledorn M, Fox TJ, Rohweder JJ, Guyon LJ, Meier AR, Cosgriff RJ, Vandermyde BJ. 2019. Spatially explicit modelling of floodplain forest succession: interactions among flood inundation, forest successional processes, and other disturbances in the Upper Mississippi River floodplain, USA. Ecological Modelling 405:15–32.

Driscoll KP, Hauer FR. 2019. Seasonal flooding affects habitat and landscape dynamics of a gravel-bed river floodplain. Freshwater Science 38:510–526.

Fahey RT, Fotis AT, Woods KD. 2015. Quantifying canopy complexity and effects on productivity and resilience in late-successional hemlock-hardwood forests. Ecological Applications 25:834–847.

Fan Y, Chen J, Shirkey G, John R, Wu SR, Park H, Shao C. 2016. Applications of structural equation modeling (SEM) in ecological studies: an updated review. Ecological Processes 5:19.

Fonseca LDM, Dalagnol R, Malhi Y, Rifai SW, Costa GB, Silva TSF, Da Rocha HR, Tavares IB, Borma LS. 2019. Phenology and Seasonal Ecosystem Productivity in an Amazonian Floodplain Forest. Remote Sensing 11.

Fotis AT, Morin TH, Fahey RT, Hardiman BS, Bohrer G, Curtis PS. 2018. Forest structure in space and time: Biotic and abiotic determinants of canopy complexity and their effects on net primary productivity. Agricultural and Forest Meteorology 250:181–191.

Glatthorn J, Feldmann E, Pichler V, Hauck M, Leuschner C. 2018. Biomass Stock and Productivity of Primeval and Production Beech Forests: Greater Canopy Structural Diversity Promotes Productivity. Ecosystems 21:704–722.

Hardiman BS, Bohrer G, Gough CM, Vogel CS, Curtisi PS. 2011. The role of canopy structural complexity in wood net primary production of a maturing northern deciduous forest. Ecology 92:1818–1827.

Hardiman BS, Gough CM, Halperin A, Hofmeister KL, Nave LE, Bohrer G, Curtis PS. 2013. Maintaining high rates of carbon storage in old forests: A mechanism linking canopy structure to forest function. Forest Ecology and Management 298:111–119.

Hauer FR, Locke H, Dreitz VJ, Hebblewhite M, Lowe WH, Muhlfeld CC, Nelson CR, Proctor MF, Rood SB. 2016. Gravel-bed river floodplains are the ecological nexus of glaciated mountain landscapes. Science Advances 2.

HEC-GeoRAS (version 10.1). 2012. US Army Corps of Engineers. http://www.hec.usace.army.mil/software/hec-georas/downloads.aspx.

HEC-RAS (version 5.0). 2016. US Army Corps of Engineers. http://www.hec.usace.army.mil/software/hec-ras/.

Helton AM, Poole GC, Meyer JL, Wollheim WM, Peterson BJ, Mulholland PJ, Bernhardt ES, Stanford JA, Arango C, Ashkenas LR, Cooper LW, Dodds WK, Gregory SV, Hall RO, Hamilton SK, Johnson SL, McDowell WH, Potter JD, Tank JL, Thomas SM, Valett HM, Webster JR, Zeglin L. 2011. Thinking outside the channel: modeling nitrogen cycling in networked river ecosystems. Frontiers in Ecology and the Environment 9:229–238.

Hershberger SL. 2001. Cause and Correlation in Biology: A User's Guide to Path Analysis, Structural Equations, and Causal Inference. Structural Equation Modeling-a Multidisciplinary Journal 8:646–649.

Hooper DU, Chapin FS, Ewel JJ, Hector A, Inchausti P, Lavorel S, Lawton JH, Lodge DM, Loreau M, Naeem S, Schmid B, Setala H, Symstad AJ, Vandermeer J, Wardle DA. 2005. Effects of biodiversity on ecosystem functioning: A consensus of current knowledge. Ecological Monographs 75:3–35.

Hooper SR, Swartz CW, Wakely MB, de Kruif REL, Montgomery JW. 2002. Executive functions in elementary school children with and without problems in written expression. Journal of Learning Disabilities 35:57–68.

Jansson R, Nilsson C, Dynesius M, Andersson E. 2000. Effects of river regulation on river-margin vegetation: A comparison of eight boreal rivers. Ecological Applications 10:203–224.

Jensen J. 2004. Introductory Digital Image Processing. Upper Saddle River, N.J.

Jenson SK, Domingue JO. 1988. Extracting topographic structure from digital elevation data for geographic information-system analysis. Photogrammetric Engineering and Remote Sensing 54:1593–1600.

Johnson SE, Amatangelo KL, Townsend PA, Waller DM. 2016. Large, connected floodplain forests prone to flooding best sustain plant diversity. Ecology 97:3019–3030.

Junk WJ, Bayley PB, Sparks RE. 1989. The flood pulse concept in river-floodplain systems. Canadian Special Publication of Fisheries and Aquatic Sciences 106:110–127.

Keeton WS, Kraft CE, Warren DR. 2007. Mature and old-growth riparian forests: Structure, dynamics, and effects on adirondack stream habitats. Ecological Applications 17:852–868.

Lane SN, Tayefi V, Reid SC, Yu D, Hardy RJ. 2007. Interactions between sediment delivery, channel change, climate change and flood risk in a temperate upland environment. Earth Surface Processes and Landforms 32:429–446.

Lane SN, Thorne CR. 2007. River processes. Thorne CR, Evans EP, Penning-Roswell EC editors. Future flooding and coastal erosion risks: ICE Publishing, ppp 82–99.

Latterell JJ, Bechtold JS, O'Keefe TC, Van Pelt R, Naiman RJ. 2006. Dynamic patch mosaics and channel movement in an unconfined river valley of the Olympic Mountains. Freshwater Biology 51:523–544.

Lillesand T, Kiefer RW, Chipman J. 2015. Remote Sensing and Image Interpretation. Hoboken, N.J.

Listopad C, Masters RE, Drake J, Weishampel J, Branquinho C. 2015. Structural diversity indices based on airborne LiDAR as ecological indicators for managing highly dynamic landscapes. Ecological Indicators 57:268–279.

Lite SJ, Bagstad KJ, Stromberg JC. 2005. Riparian plant species richness along lateral and longitudinal gradients of water stress and flood disturbance, San Pedro River, Arizona, USA. Journal of Arid Environments 63:785–813.

Lorang MS, Whited DC, Hauer FR, Kimball JS, Stanford JA. 2005. Using airborne multispectral imagery to evaluate geomorphic work across floodplains of gravel-bed rivers. Ecological Applications 15:1209–1222.

Luck M, Maumenee N, Whited D, Lucotch J, Chilcote S, Lorang M, Goodman D, McDonald K, Kimball J, Stanford J. 2010. Remote sensing analysis of physical complexity of North Pacific Rim rivers to assist wild salmon conservation. Earth Surface Processes and Landforms 35:1330–1343.

Mac Nally R, Cunningham SC, Baker PJ, Horner GJ, Thomson JR. 2011. Dynamics of Murray-Darling floodplain forests under multiple stressors: The past, present, and future of an Australian icon. Water Resources Research 47.

Mahoney JM, Rood SB. 1998. Streamflow requirements for cottonwood seedling recruitment - An integrative model. Wetlands 18:634–645.

Malard F, Tockner K, Ward JV. 1999. Shifting dominance of subcatchment water sources and flow paths in a glacial floodplain (Val Roseg, Switzerland). Arctic, Antarctic and Alpine Research 31:135–150.

McCallum K, Beaty M, Mitchell B. 2014. First Order Lidar Metrics: A Supporting Document For Lidar Deliverables. Salt Lake City, UT: U.S. Department of Agriculture, Forest Service, Remote Sensing Applications Center.

Megonigal JP, Conner WH, Kroeger S, Sharitz RR. 1997. Aboveground production in Southeastern floodplain forests: A test of the subsidy-stress hypothesis. Ecology 78:370–384.

Mertes LAK. 2002. Remote sensing of riverine landscapes. Freshwater Biology 47:799–816.

Naeem S, Hakansson K, Lawton JH, Crawley MJ, Thompson LJ. 1996. Biodiversity and plant productivity in a model assemblage of plant species. Oikos 76:259–264.

Naeem S, Thompson LJ, Lawler SP, Lawton JH, Woodfin RM. 1994. Declining biodiversity can alter the performance of ecosystems. Nature 368:734–737.

Naiman RJ, Bechtold JS, Beechie TJ, Latterell JJ, Van Pelt R. 2010. A Process-Based View of Floodplain Forest Patterns in Coastal River Valleys of the Pacific Northwest. Ecosystems 13:1–31.

Naiman RJ, Bilby RE, Schindler DE, Helfield JM. 2002. Pacific salmon, nutrients, and the dynamics of freshwater and riparian ecosystems. Ecosystems 5:399–417.

Naiman RJ, Decamps H, McClain ME. 2005. Riparia: ecology, conservation and management of streamside communities. Sand Diego: Elsevier/Academic Press.

Odum EP, Finn JT, Franz EH. 1979. Perturbation-theory and the subsidy-stress gradient. Bioscience 29:349–352.

Papadimitriou F. 2002. Modelling indicators and indices of landscape complexity: An approach using G.I.S. Ecological Indicators - 2.

Parsons M, Thoms MC. 2013. Patterns of vegetation greenness during flood, rain and dry resource states in a large, unconfined floodplain landscape. Journal of Arid Environments 88:24–38.

Pettit NE, Naiman RJ, Warfe DM, Jardine TD, Douglas MM, Bunn SE, Davies PM. 2017. Productivity and Connectivity in Tropical Riverscapes of Northern Australia: Ecological Insights for Management. Ecosystems 20:492–514.

Pollock MM, Naiman RJ, Hanley TA. 1998. Plant species richness in riparian wetlands - A test of biodiversity theory. Ecology 79:94–105.

Quinn GP, Keough MJ. 2002. Experimental design and data analysis for biologists: Cambridge University Press.

R Development Core Team. 2008. R: A language and environment for statistical computing. Computing RFfS editor. Vienna, Austria.

Records RM, Wohl E, Arabi M. 2016. Phosphorus in the river corridor. Earth-Science Reviews 158:65–88.

Robertson AI, Bacon P, Heagney G. 2001. The responses of floodplain primary production to flood frequency and timing. Journal of Applied Ecology 38:126–136.

Rood SB, Samuelson GM, Braatne JH, Gourley CR, Hughes FMR, Mahoney JM. 2005. Managing river flows to restore floodplain forests. Frontiers in Ecology and the Environment 3:193–201.

Rosseel Y. 2012. lavaan: An R package for structural equation modeling. J Stat Softw: 1–36.

Running SW, Nemani RR, Heinsch FA, Zhao M, Reeves M, Hashimoto H. 2004. A continuous satellite-derived measure of global terrestrial primary production. BioScience 54:547–560.

Saatchi SS, Houghton RA, Alvala R, Soares JV, Yu Y. 2007. Distribution of aboveground live biomass in the Amazon basin. Global Change Biology 13:816–837.

Salo J, Kalliola R, Hakkinen I, Makinen Y, Niemela P, Puhakka M, Coley PD. 1986. River dynamics and the diversity of amazon lowland forest. Nature 322:254–258.

Schindler DE, Smits AP. 2017. Subsidies of Aquatic Resources in Terrestrial Ecosystems. Ecosystems 20:78–93.

Scown MW, Thoms MC, De Jager NR. 2016. An index of floodplain surface complexity. Hydrology and Earth System Sciences 20:431–441.

Siegloch AE, Schmitt R, Spies M, Petrucio M, Hernandez MIM. 2017. Effects of small changes in riparian forest complexity on aquatic insect bioindicators in Brazilian subtropical streams. Marine and Freshwater Research 68:519–527.

Sobel ME. 1982. Asymptotic Confidence Intervals for Indirect Effects in Structural Equation Models. Sociological Methodology 13:290–312.

Stanford JA, Lorang MS, Hauer FR. 2005. The shifting habitat mosaic of river ecosystems. Verhandlungen Internationale Vereinigung Für Theoretische Und Angewandte Limnologie 29:123–136.

Stella J, Hayden M, Battles J, Piegay H, Dufour S, Fremier AK. 2011. The Role of Abandoned Channels as Refugia for Sustaining Pioneer Riparian Forest Ecosystems. Ecosystems 14:776–790.

Streng DR, Glitzenstein JS, Harcombe PA. 1989. Woody seedling dynamics in an east texas floodplain forest. Ecological Monographs 59:177–204.

Swanson W, De Jager NR, Strauss E, Thomsen M. 2017. Effects of flood inundation and invasion by Phalaris arundinacea on nitrogen cycling in an Upper Mississippi River floodplain forest. Ecohydrology 10.

Tarboton DG, Bras RL, Rodriguez-Iturbe I. 1991. On the extraction of channel networks from digital elevation data. Hydrological Processes 5:81–100.

Thapa R, Thoms M, Parsons M. 2016. An adaptive cycle hypothesis of semi-arid floodplain vegetation productivity in dry and wet resource states. Ecohydrology 9:39–51.

Thevs N, Buras A, Zerbe S, Kuhnel E, Abdusalih N, Ovezberdiyeva A. 2012. Structure and wood biomass of near-natural floodplain forests along the Central Asian rivers Tarim and Amu Darya. Forestry 85:193–202.

Tilman D, Knops J, Wedin D, Reich P, Ritchie M, Siemann E. 1997. The influence of functional diversity and composition on ecosystem processes. Science 277:1300–1302.

Tilman D, Wedin D, Knops J. 1996. Productivity and sustainability influenced by biodiversity in grassland ecosystems. Nature 379:718–720.

Tockner K, Lorang MS, Stanford JA. 2010. River flood plains are model ecosystems to test general hydrogeomorphic and ecological concepts. River Research and Applications 26:76–86.

Tockner K, Stanford JA. 2002. Riverine flood plains: present state and future trends. Environmental Conservation 29:308–330.

Tucker CJ. 1979. Red and photographic infrared linear combinations for monitoring vegetation. Remote Sensing of Environment 8:127–150.

Ahl R., Brown S. 2017. The Bitterroot and Lolo National Forests Region 1 Existing Vegetation Database (VMap) Revision of 2016. USDA Forest Service. Nothern Region Geospatial Group (NRGG). Project Report : NRGG_PR_BITLO_VMAP2016

Valett HM, Hauer FR, Stanford JA. 2014. Landscape Influences on Ecosystem Function: Local and Routing Control of Oxygen Dynamics in a Floodplain Aquifer. Ecosystems 17:195–211.

von Gadow K, Zhao XH, Tewari VP, Zhang CY, Kumar A, Rivas JJC, Kumar R. 2016. Forest observational studies: an alternative to designed experiments. European Journal of Forest Research 135:417–431.

Vuong QH. 1989. Likelihood ratio tests for model selection and non-nested hypotheses. Econometrica 57:307–333.

Ward JV, Tockner K, Schiemer F. 1999. Biodiversity of floodplain river ecosystems: ecotones and connectivity. Regulated Rivers: Research & Management 15:125–139.

Ward JV, Tockner K, Arscott DB, Claret C. 2002. Riverine landscape diversity. Freshwater Biology 47:517–539.

Warren DR, Keeton WS, Kiffney PM, Kaylor MJ, Bechtold HA, Magee J. 2016. Changing forests-changing streams: riparian forest stand development and ecosystem function in temperate headwaters. Ecosphere 7.

Whited DC, Lorang MS, Harner MJ, Hauer FR, Kimball JS, Stanford JA. 2007. Climate, hydrologic disturbance, and succession: Drivers of floodplain pattern. Ecology 88:940–953.

Wittmann F, Schongart J, Montero JC, Motzer T, Junk WJ, Piedade MTF, Queiroz HL, Worbes M. 2006. Tree species composition and diversity gradients in white-water forests across the Amazon Basin. Journal of Biogeography 33:1334–1347.

Wohl E, Hall RO, Lininger KB, Sutfin NA, Walters DM. 2017. Carbon dynamics of river corridors and the effects of human alterations. Ecological Monographs 87:379–409.

Yarie J. 2008. Effects of moisture limitation on tree growth in upland and floodplain forest ecosystems in interior Alaska. Forest Ecology and Management 256:1055–1063.